Junttila *et al.* Supplemental Figure 1

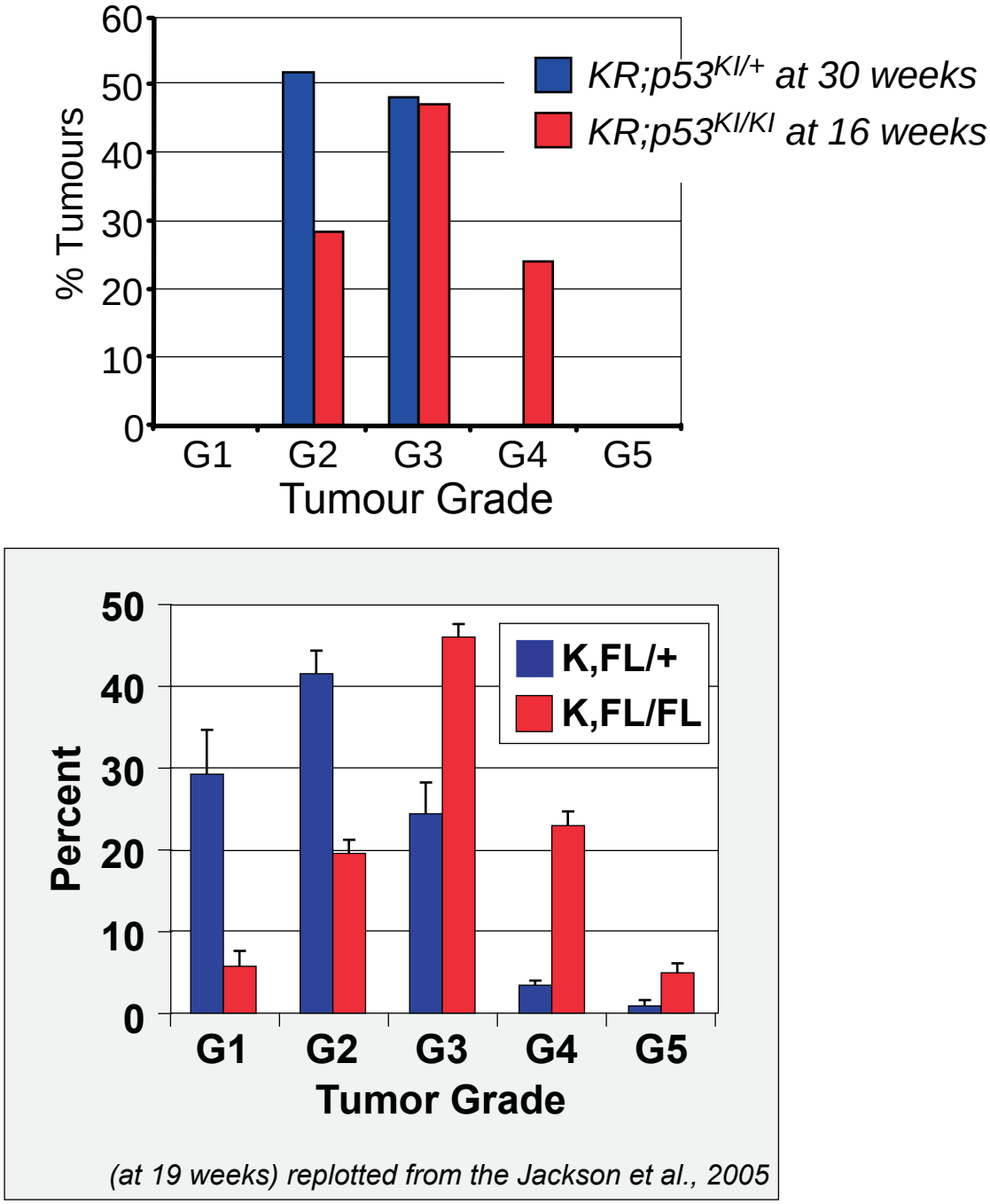

Figure S1. Kinetics of lung tumour progression in *KR;p53$^{KI/KI}$* mice is accelerated relative to p53-competent mice and similar to that published for p53 null tumours
The tumour spectra in *KR;p53$^{KI/KI}$* and *KR;p53$^{KI/+}$* mice were compared to each other and those reported for KR;p53-deficient mice (Jackson *et al.,* 2005) [6], using the same grading parameters. Only a small number of grade 3 tumours were detectable in *KR;p53$^{KI/+}$* mice 16 weeks after Kras activation. Therefore, to increase the multiplicity and grade of lesions, tumours from *KR;p53$^{KI/+}$* mice were collected at 30 weeks. (*KR;p53$^{KI/KI}$* n=91; *KR;p53$^{KI/+}$* n=110 tumours).

Junttila *et al.* Supplemental Figure 2

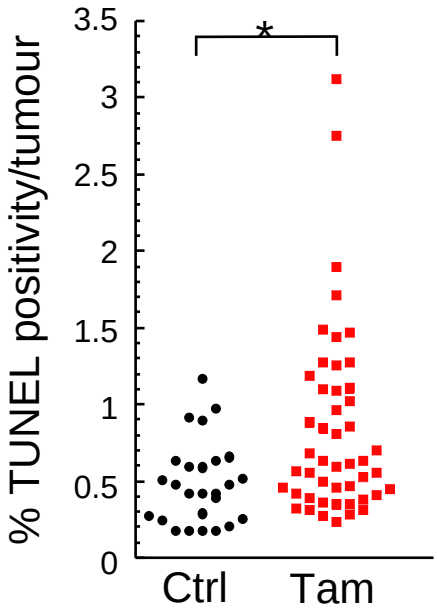

Figure S2. Heterogeneous apoptotic response of individual tumours to p53 restoration

Quantitative analysis of TUNEL positive tumours 16 weeks after adenoviral-Cre inocculation. Tumour-bearing *KR;p53$^{KI/KI}$* mice were treated for 6 hrs with either vehicle (Ctrl, n=26) or Tam (n=49) 16 weeks after adenoviral infection The y-axis indicates the percent of total cells in each tumour that are TUNEL-positive. Each circle/square represents an individual tumour. *P=0.005, Wilcoxon Rank Sum.

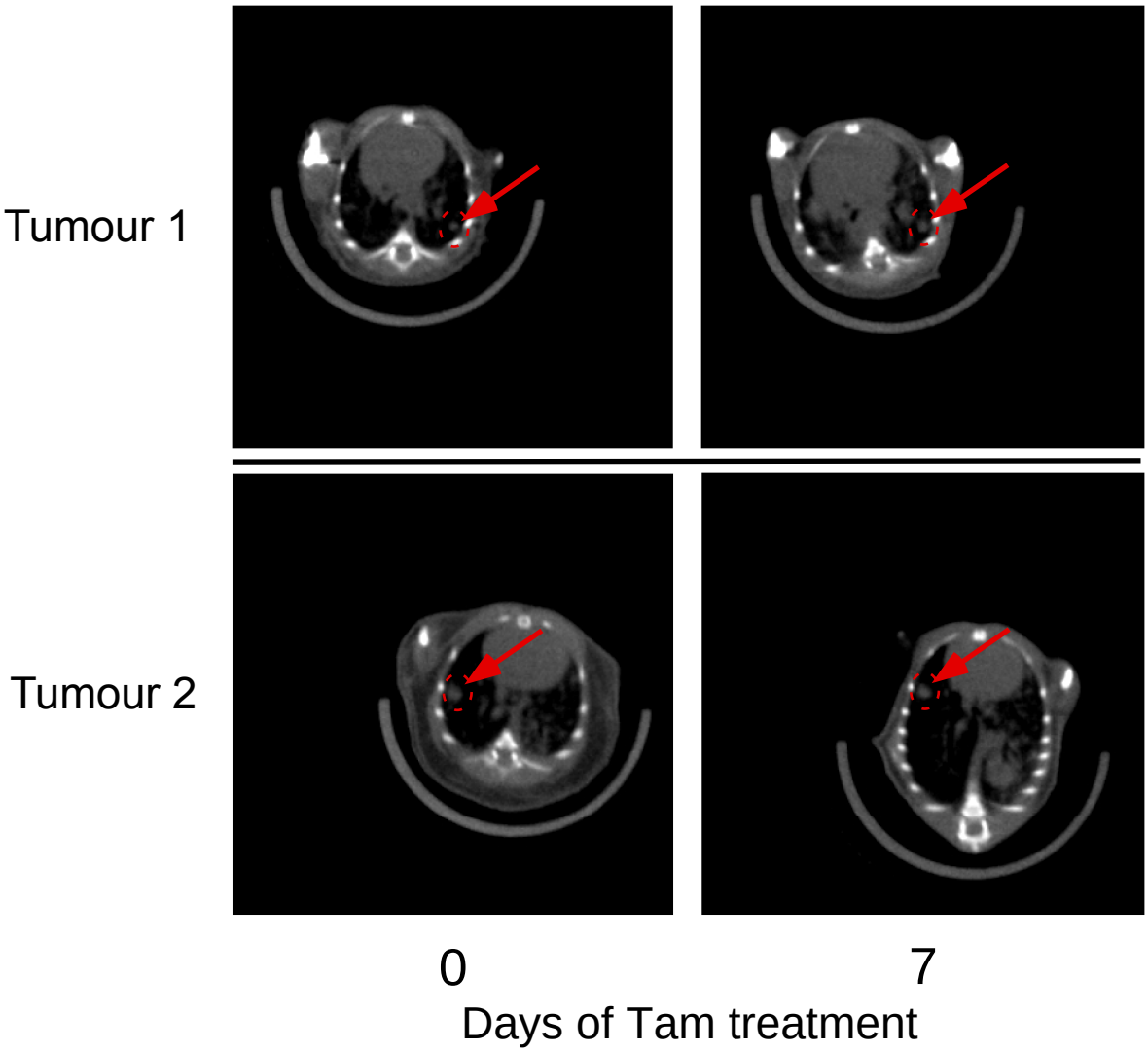

Figure S3. Micro CT analysis of individual tumours pre- and post-treatment
Representative transaxial micro CT views of pre- and post-therapy images of *KR;p53*$^{KI/KI}$ lung tumours. The upper panel shows a tumour that doubles in size (1.9 fold increase in tumour volume) and the lower panel is an example of a tumour that decreased in size (from 1 to 0.7). Left panel, day 0 (before initial Tamoxifen treatment); right panel, day 7 (following 7 daily Tam treatments). Arrows indicate the same tumour at these time points.

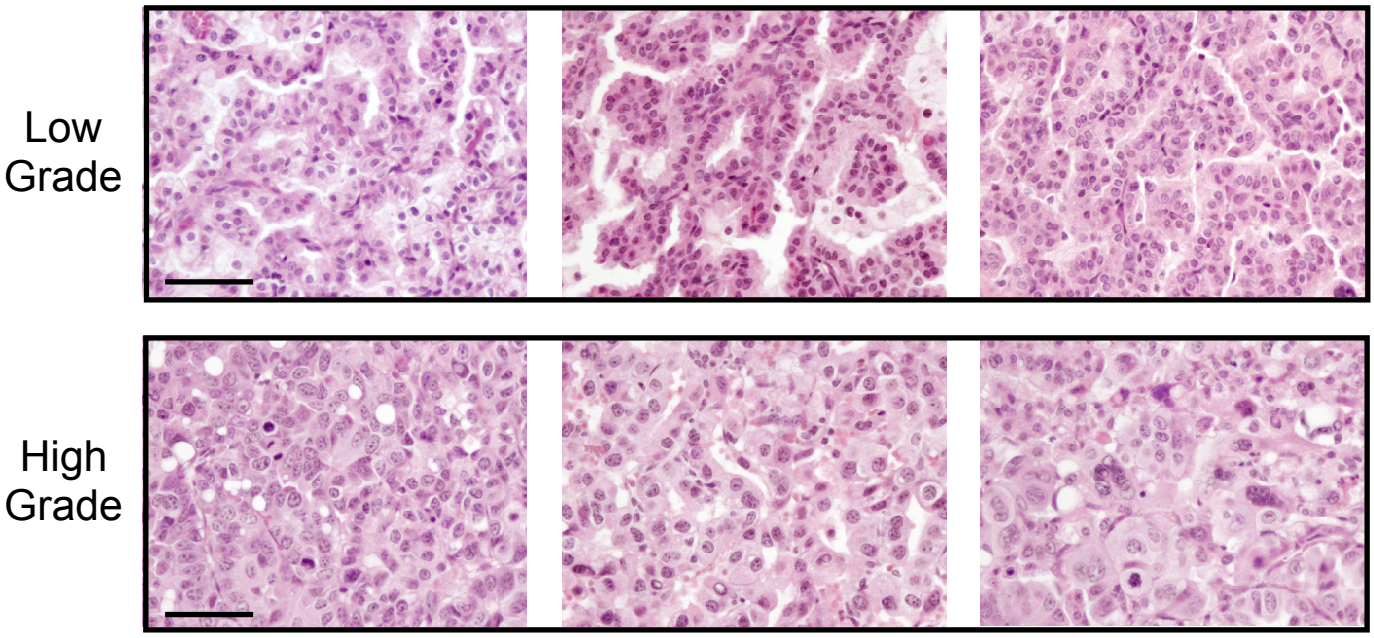

Figure S4. Tumour grading template in *KR;p53$^{KI/KI}$* mice
Haematoxylin and eosin-stained sections from three independent, representative lung tumours are presented to illustrate the principles used to designate the histological grade of tumours based on degree of nuclear atypia. Tumour classification followed the general guidelines proposed by Nikitin and colleagues [20] and stratifies tumours in grades 1-3. Here, to simplify the analysis, grade 1 and 2 tumours were grouped together as "Low grade" tumours while grade 3 tumours were grouped as "High grade." Tumours retaining alveolar architecture with bronchioloalveolar-type or papillary growth pattern, and showing no definitive evidence of invasion, were classed as adenomas: the great majority of these tumours exhibited low-grade nuclear features. Tumours exhibiting indistinct alveolar architecture, extensive solid or acinar growth pattern or stromal desmoplasia, were classed as adenocarcinomas. Almost all adenocarcinomas were classified as high grade tumours and appeared to arise either ab initio or by cladal evolution from within a low grade adenoma. Scale bars = 50 µm.

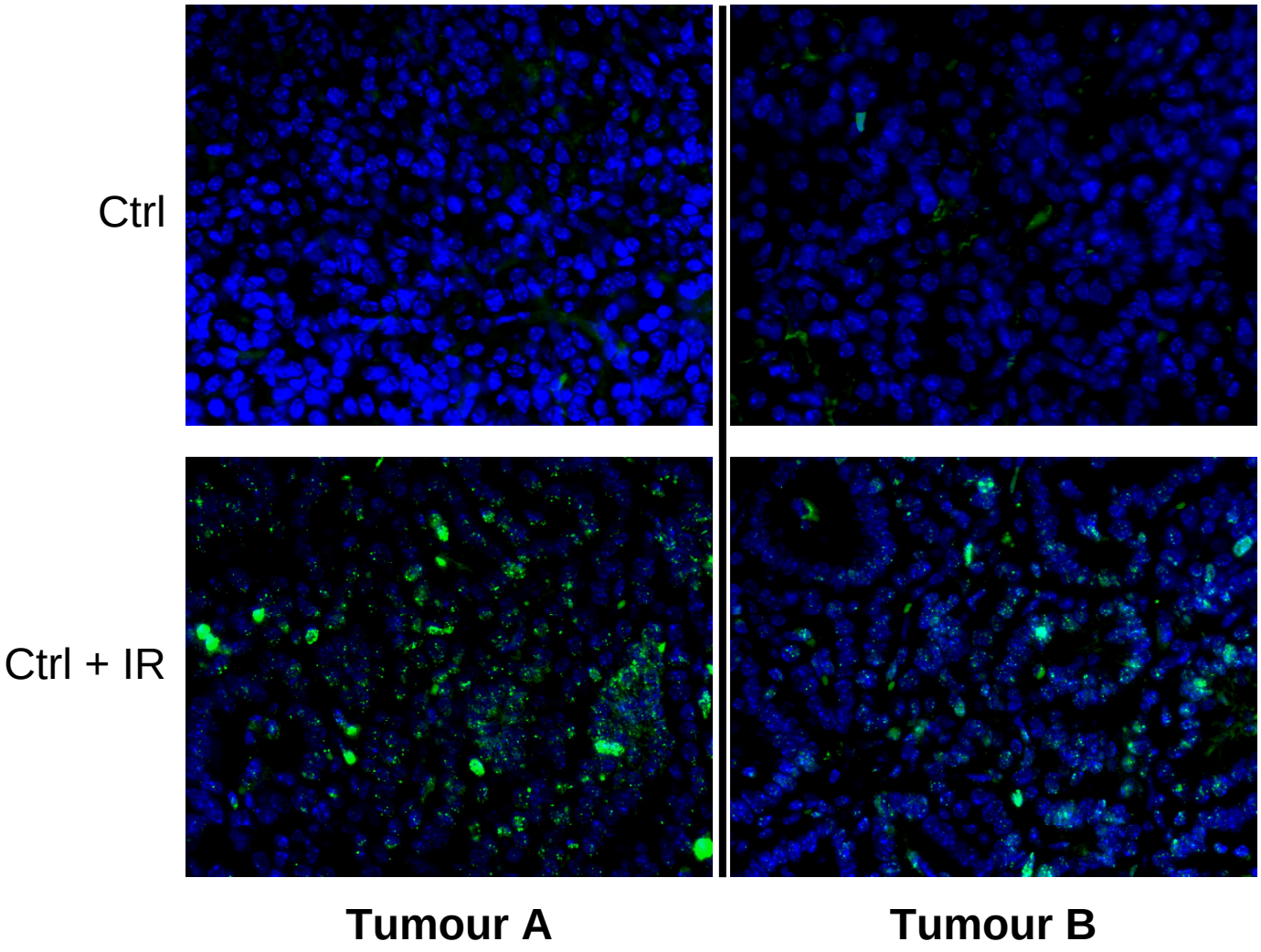

Figure S5. ***KR;p53$^{KI/KI}$*** **tumours exhibit negligible ongoing endogenous DNA damage**
Immunofluorescence staining for the DNA damage marker γ-H2AX expression levels in two representative lung tumours from *KR;p53$^{KI/KI}$* mice treated with vehicle alone (Ctrl - upper panels) or in combination with 4 Gy whole body γ-irradiation (Ctrl + IR - lower panels).

Junttila *et al.* Supplemental Figure 6

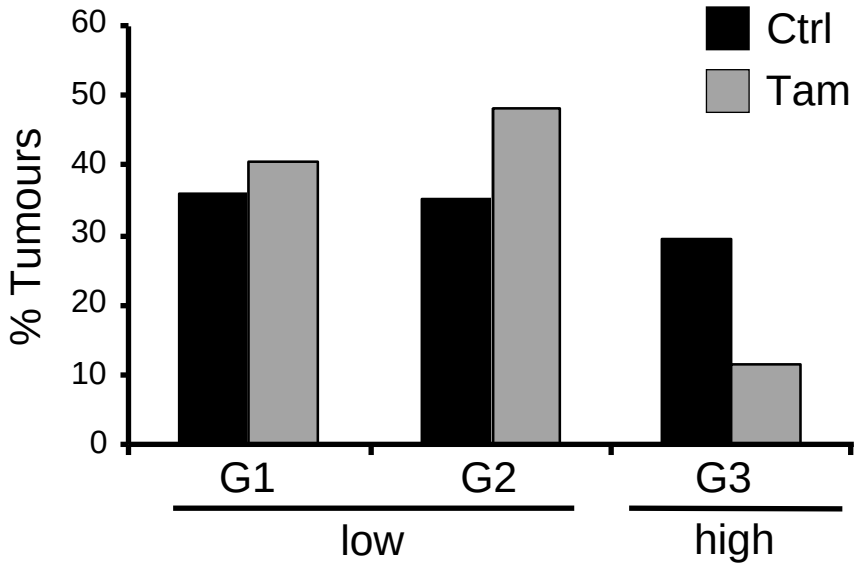

Figure S6. Restoration of p53 function reduces the relative proportion of *KR;p53$^{KI/KI}$* tumours assigned as grade 3 (high grade)

Quantification of the frequency of each tumour grade in lungs of *KR;p53$^{KI/KI}$* mice treated for 7 days with either control vehicle (Ctrl) or Tamoxifen (Tam) to restore p53 function. Data are presented as percent of total tumours in each grade (n = 143 Ctrl; n = 163 Tam).

Junttila *et al*., Supplemental Figure 7

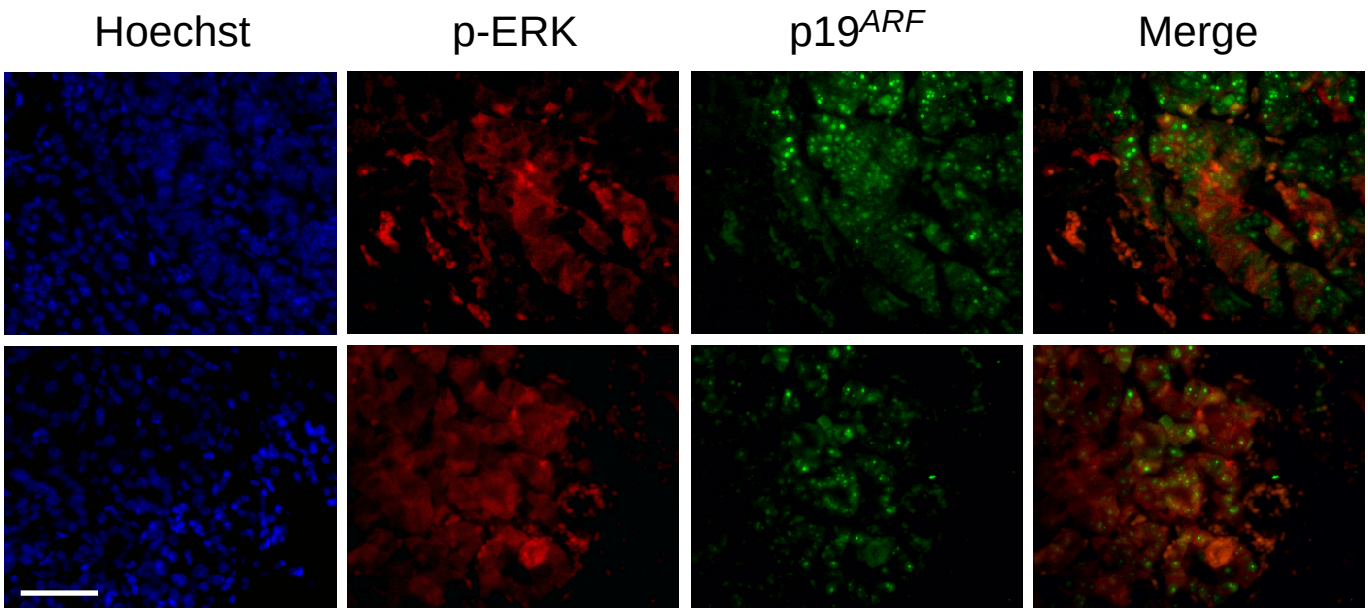

Figure S7. p53-responsive tumour cells exhibit elevated Kras signalling
Co-immunostaining for $p19^{ARF}$ and p-ERK in two independent tumours from sham-treated *KR;p53*$^{KI/KI}$ mice, showing that expression of $p19^{ARF}$ and high p-ERK co-localize at the individual cell level. Scale bar = 50 µm.

Junttila *et al*., Supplemental Figure 8

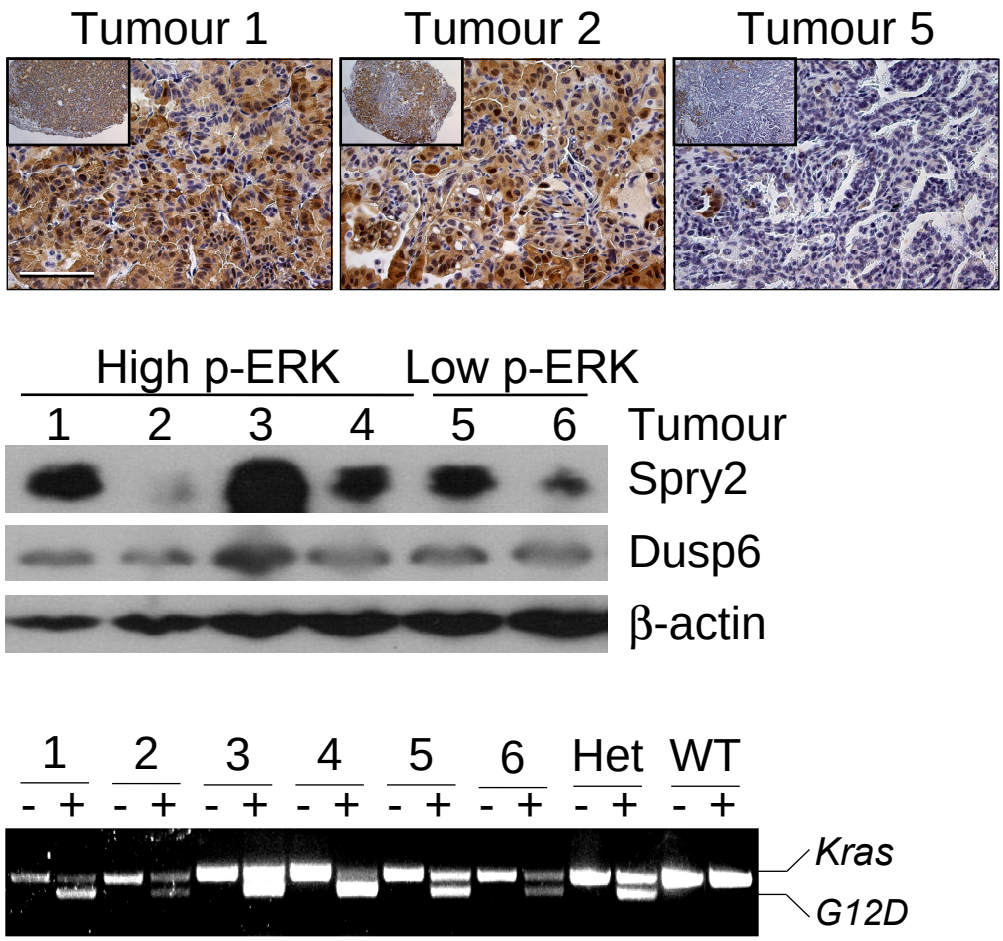

Figure S8. Sprouty 2 loss and wt/mutant Kras allele imbalance in high p-ERK lung tumours

To investigate potential mechanisms for Kras signal up regulation in high-grade tumours, individual low and high grade tumours were collected and each divided in half - one half used for IHC and the other for protein/DNA analysis. Lysates from tumours stratified as low (tumours 5 and 6) or high (tumours 1-4) p-ERK (illustrated in the upper panels, scale bar = 50 μm) were analyzed by immunoblotting (middle panel) for expression of Sprouty2 (Spry2), Dusp6 and β-actin (loading control). DNA from the same tumours was extracted and the Kras genomic region amplified by PCR (lower panel) and digested with HindIII, which allows for discrimination between wt (Kras, upper band) and mutant alleles (G12D, lower band). Undigested (-) and digested (+) DNA were then run alongside in pairs. wt/wt (WT) and heterozygous wt/$Kras^{G12D}$ DNAs (Het) were used as control. No significant differences in Dusp6 expression were found in high versus low p-ERK tumours: however, one high p-ERK tumour (#2) exhibited marked down-regulation of Sprouty2. Relative gene copy level analysis of wt Kras and mutant $Kras^{G12D}$ alleles from genomic tumour DNA indicated significant overall Kras copy number imbalance favouring the mutant $Kras^{G12D}$ allele in 2/4 “high” p-ERK tumours.

Junttila *et al*., Supplemental Figure 9

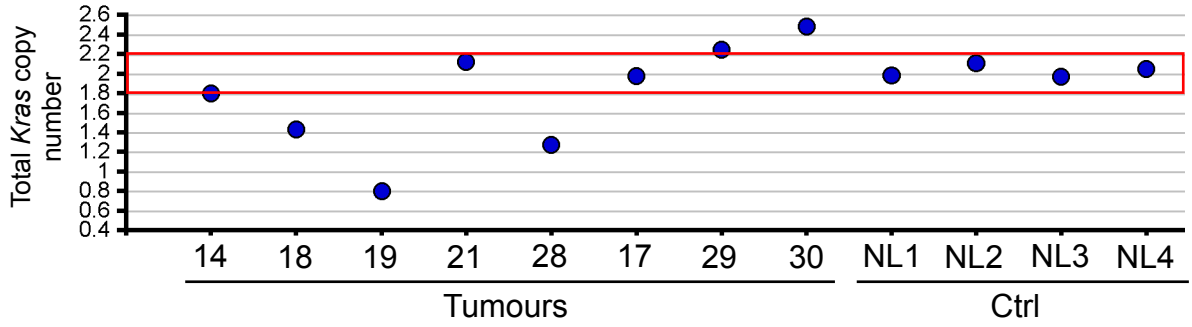

Figure S9. wt Kras loss and mutant allele duplication in high p-ERK regions of lung tumours

To confirm that the abnormally high $Kras^{G12D/}Kras^{wt}$ Kras ratios in high p-ERK tumour tissues is due to actual loss of wt Kras (rather than overwhelming amplification of the mutant $Kras^{G12D}$ and concomitant relative under-representation of the wt Kras allele), genomic DNA from a representative subset of low, mixed and high p-ERK tumour regions was isolated and total Kras gene copy number (wt plus mutant) quantified by Taqman. While tumours differed somewhat in their overall Kras gene content (average value: 1.7, SD=0.4), no significant amplification (greater than or equal to 3 copies) of Kras alleles was evident in any sample. Of note, samples harbouring overall greater than or equa to 2 Kras alleles but with no wt Kras allele have presumably duplicated their mutant Kras allele. Also of note, tumour 14 (“Low” p-ERK) has a Kras copy number value close to 2 (1.8), indicating that both alleles are present and neither is amplified. NL controls are derived from normal lung tissue.